

# Fabrication of ZnO Nanoparticles for Photocatalytic Reduction of CO<sub>2</sub>

Guang NI<sup>1,a</sup>, Yinfei CHEN<sup>1,b</sup>, Yulan LIU<sup>1,c</sup>, Huayan LIU<sup>1,d</sup>, and Zekai ZHANG<sup>1,e\*</sup>

<sup>1</sup>College of Chemical Engineering, Zhejiang University of Technology, Chaowang road 18, 310014 Hangzhou, China

<sup>a</sup>bbmmjlp@126.com, <sup>b</sup>yfchen@zjut.edu.cn, <sup>c</sup>lyl\_edu@126.com, <sup>d</sup>hyliu@zjut.edu.cn, <sup>e</sup>zzk@zjut.edu.cn

**Abstract.** ZnO nanoparticles were fabricated by anodization method. Different fabrication conditions, including pH buffers (sodium hydroxide, citric acid, oxalic acid, hydrogen peroxide), electrolyte concentration, temperature and voltage were investigated. The field emission scanning electron microscopes (FESEMs) revealed that zinc oxide nanoparticles with discal morphology were formed. The optimum conditions for fabrication of nano ZnO material with discal shape nanoparticles are 1wt% NH<sub>4</sub>F electrolyte in water ethano(1:1) solution at 25°C and 40v with 0.2M citric acid as pH buffer. This ZnO material shows rather high photocatalytic reduction activity of CO<sub>2</sub> and the yield of CH<sub>4</sub> reaches 2.48 umol/g catalyst.

**Keywords:** Zinc oxide nanoparticles, discal morphology, preparation conditions, photocatalytic reduction

## 1 Introduction

Zinc oxide has drawn considerable attention because of its attractive optical-electrical characteristics[1,2] that make it potentially applicable in a lot of fields such as ultraviolet lasing[3], photocatalysts[4]and so on[5,6]. In addition, 1D nanoscale ZnO is preferred in photoanode applications due to its larger surface area[7].

Anodic oxidation has been employed in synthesis of many kinds of metal oxides with 1D nanostructure[8~10]. Research on anodization of various valve metals by P. Schmuki group[11~14] showed that anodizing can be applied to the preparation of nanostructures of other valve metals. Anodization of Zn that is one of the valve metals especially synthesis of 1D nanoscale of ZnO by anodizing has been widely investigated, since its gentle conditions and cheap equipment. S. Sreekantan et al.[7] have reported that nanoneedle, nanoflower and nanoflake of ZnO can be obtained by anodization in different concentration of sodium hydroxide. Apiked ZnO nanowire structures[15] are achieved by changing the NH<sub>4</sub>F concentration. Studies on the preparation of ZnO strips have been conducted by Sung Joong Kim et al[16].

Although many researches have concentrated on 1D nanoscale ZnO, research of various nanostructures in this field is still at primary stage. Hence, the new morphology and application of ZnO nanoparticle is yet to be further found. The key to nanostructure of ZnO

\* Corresponding author: zzk@zjut.edu.cn

synthesized by anodizing is the balance of the formation and dissolution of ZnO. It is known that anodic zinc oxide is very easily dissolved in strong acidic or basic conditions[17]. In this paper, we prepared ZnO nanoparticles with discal morphology by carefully adjustment of pH buffer and other conditions. This ZnO material is supposed to be good for application of photoelectricity due to its regular structures such as large absorption area and flat surface beneficial to electronic transmission. The influence of preparation conditions such as electrolyzer、temperature, voltage, etc are explored in detail. Furthermore, its photocatalytic reduction activity of CO<sub>2</sub> is conducted and its yield of CH<sub>4</sub> is observed.

## 2 Experimental

Zinc foils (20-mm thickness) with a purity of 99.99% were purchased from Qingyuan company of metal materials. A zinc plate with size of 20\*40\*0.02mm was cleaned with acetone and ethanol in an ultrasonic bath for 10min. Subsequently, to remove the oxide layer on the surface, it was polished by the NaOH solution of concentration 0.3mol/l, washed with ethanol 3-5 times and dried with a stream of N<sub>2</sub> gas. The anodization was carried out by using a two-electrode system consisting of the zinc foil and a platinum foil as anode and cathode, respectively. The distance between anode and cathode was 50 mm. At the first stage, anodic etching was conducted in 1wt% NH<sub>4</sub>F aqueous solution with different pH buffer (sodium hydroxide, citric acid, oxalic acid, hydrogen peroxide) at 25°C and 40V for 10 min. Next, different anodization conditions including electrolyte (H<sub>2</sub>O, H<sub>2</sub>O:C<sub>2</sub>H<sub>5</sub>OH 1:1, H<sub>2</sub>O: glycol 1:1), temperature (25,35,45°C), voltage (40,50,60v) and NH<sub>4</sub>F quality score (0.5%,1%,1.5%) are investigated. The stirring rate was kept constant during the anodization.

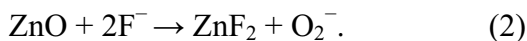
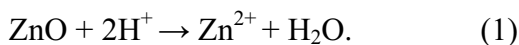
The morphology and composition of anodic zinc oxides were characterized by a field emission scanning electronmicroscope (FE-SEM, Hitachi S-4700, Japan), operated at an accelerating voltage of 15 kV.

Photocatalytic reduction of CO<sub>2</sub> was conducted in a sealed stainless steel reactor having a quartz window through which the sample can be exposed to light. The reaction system contains 0.1MPa CO<sub>2</sub> and 2ml H<sub>2</sub>O. A 300-W Xe lamp is light source. The weight of anodic zinc oxides is about 0.01g. Reaction products were analyzed by a Techcompa gas chromatograph (GC7900) equipped with thermal conductivity detector and a Shimadzu gas chromatograph (GC-2014) equipped with flame ionization detector.

## 3 Results and Discussion

### 3.1 Feature of Anodic Zinc Oxide

The morphologies of ZnO obtained by anodic dissolution with different pH buffer (sodium hydroxide, citric acid, oxalic acid, hydrogen peroxide ) for 1 min are shown in Fig. 1. It is nature to find that the shape of ZnO depends on the types of the pH buffer, as it has been reported that zinc oxide can exist neither in strong acidic nor basic conditions[17]. Layers of anodic zinc oxide come out with the addition of hydrogen peroxide (Fig. 1a). The layers of ZnO are finally formed by ZnO nanoparticles from the reaction of hydroxide ions and Zn<sup>2+</sup> ions at the initial stage[18]. Fig. 1b, 1c and 1d show that the smaller concentration of hydrogen ion, the more regular ZnO nanoparticles. It can be explained by this reaction as follows [16,19]:



Reaction (1) can aggravate the dissolution of ZnO nanoparticles, as disk-like nanoparticles presented in Fig. 1c and Fig. 1d. Appropriate concentration of hydrogen ion may be favorable for the balance between generation and dissolution. The amount and the uniformity of the ZnO nanoparticles prepared with 0.2M citric acid (Fig. 1d) is the optimum.

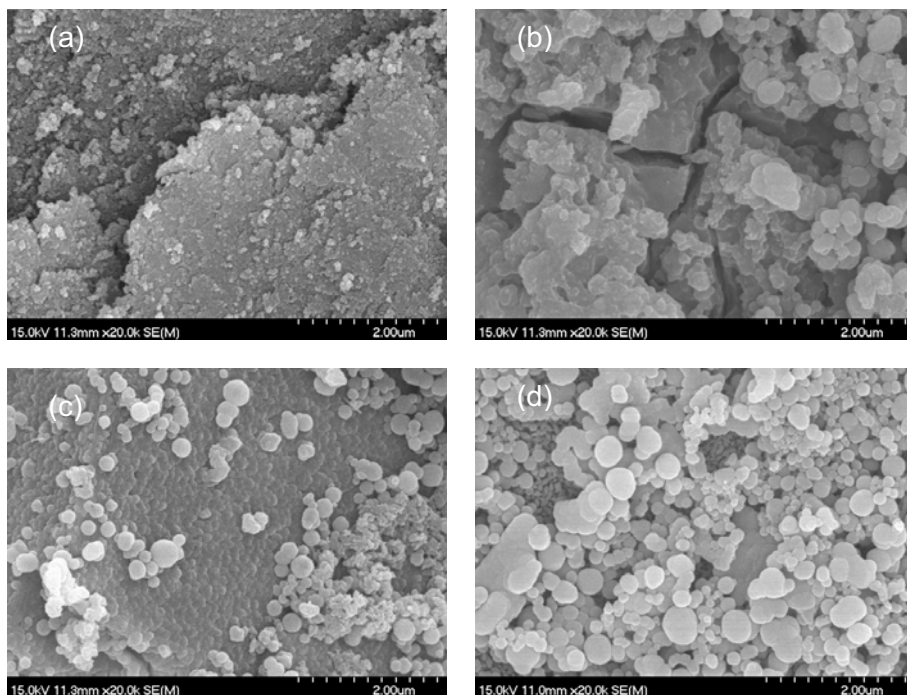


**Fig. 1.** FE-SEM images of the ZnO prepared with different pH regulators. (a)0.2M hydrogen peroxide, (b) 0.2M oxalic acid, (c) 0.2M sodium hydroxide and (d)0.2M citric acid.

### 3.2 Effect of the Electrolyzer on the Morphology of ZnO

The effect of the electrolyzer reflects in blocking on the movement speed of ions[20]. Similar to the process of anodic etching of Ti foil, there are two layers in the vertical attitude of Zn foil, as described in the Fig. 2d. The upper layer consists of ZnO while the under is composed of unreacted Zn. Two reaction steps, namely the generation and the dissolution of nano-ZnO, determine the morphology of the oxide layer of ZnO during anodizing. Surface morphology of ZnO layer in different electrolyzer are shown in Fig. 2a, b and c. It can be observed that the composition of electrolyte plays an important role on

the degree of the uniformity of the ZnO layer. Cracks can be seen everywhere on the surface in pure H<sub>2</sub>O (Fig. 2.a) and the surface in glycol/H<sub>2</sub>O electrolyzer is much rough and uneven by random etching (Fig. 2.c). Meanwhile, the surface of ZnO is uniform in ethanol/H<sub>2</sub>O ((Fig. 2.b). Further, nanoparticles with disc-like shape can be seen in all of the enlarged images (the inset micrograph in Fig.3.a, b and c). The distribution and the shapes of ZnO nanoparticles in the Fig.2b are also more uniform and clearer than the other two samples, which indicates that the stable anodization in ethanol/H<sub>2</sub>O electrolyzer.

The effect of electrolyzer may be originated from the difference in viscosity or the movement speed of H<sup>+</sup>, F<sup>-</sup> and NH<sub>4</sub><sup>+</sup> ions, which will influence the generation and the dissolution rates of nano-ZnO. Appropriate viscosity can cause proper movement speed and the uniform surface come into being. According to research before, the movement of ions in solution can simplified as two-orientation strength model (Fig.3d), of which one is parallel to the face of anode, the other is vertical to it. The parallel strength contributes to concentration distribution while the vertical to generation/dissolution of ZnO nanoparticles. Pure water has little viscosity that the vertical strength dominates the anodization process, leading to fast etching of ZnO nanoparticles (Fig.3a). On the contrary, the proper viscosity of ethanol/H<sub>2</sub>O brings the uniformity(Fig.3b).

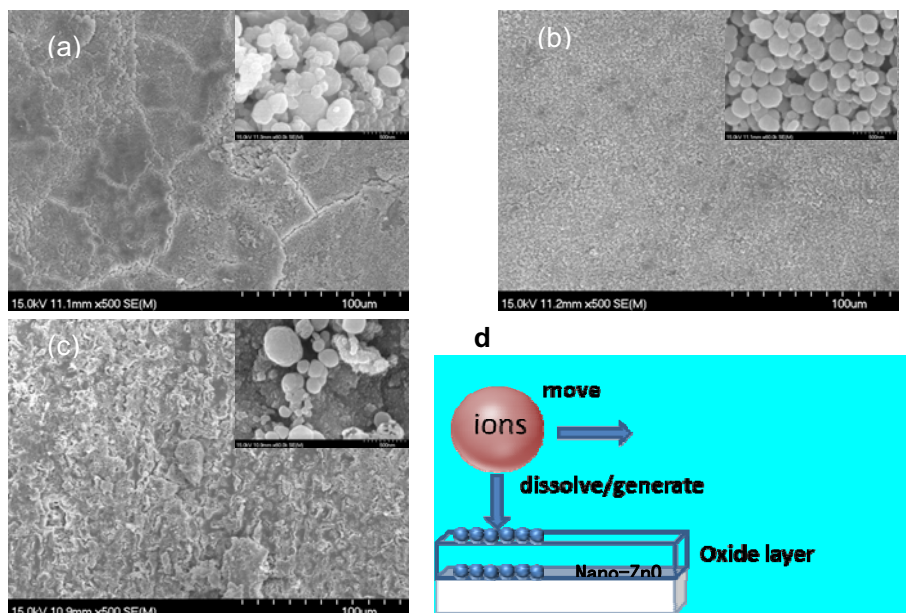


**Fig. 2.** FE-SEM images of ZnO layer prepared with different electrolyzer. (a) pure H<sub>2</sub>O, (b) H<sub>2</sub>O:C<sub>2</sub>H<sub>5</sub>OH 1:1,(c) H<sub>2</sub>O: glycol 1:1. (d) the scheme of Zn anodizing

### 3.3 Effect of NH<sub>4</sub>F Concentration on the Morphology of ZnO

NH<sub>4</sub>F concentration plays a key role in controlling the surface morphology. Different concentrations cause the different nanostructures on the surface. Low concentration of NH<sub>4</sub>F leads to ZnO nanosheets(Fig. 3a) while high concentration forms discal ZnO nanoparticles. Reaction (3) can help us to understand this interesting phenomenon. It can be seen that the competitive reactions of the generation and the dissolution of ZnO determine the growth speed and the morphology of nano-ZnO. At low NH<sub>4</sub>F concentration, the

amounts of ions is not enough to break the ZnO layer into pieces (nanoparticles) and the nanosheets come into being. If the concentration of  $\text{NH}_4\text{F}$  is too high, excessive ions will increase the dissolution rate of the nano-ZnO species and only left tiny ZnO particles.

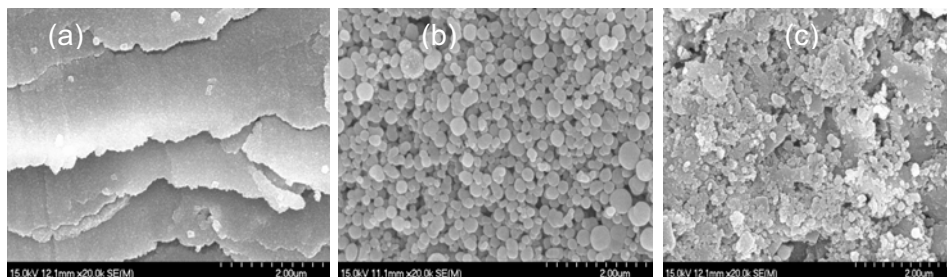


**Fig.3.** FE-SEM images of nano-ZnO prepared with different  $\text{NH}_4\text{F}$ . (a) 0.5% $\text{NH}_4\text{F}$  (b) 1% $\text{NH}_4\text{F}$  (c) 1.5% $\text{NH}_4\text{F}$ .

### 3.4 Effect of Temperature and Reactive Voltage on the Morphology of ZnO

Other anodization conditions, such as the temperature and the reactive voltage, also can affect the balance between the two reactions and the final ZnO morphologies. The results are shown in Fig. 4 and Fig.5. With the reaction temperature increases, the shapes of ZnO nanoparticles changes to be irregular and the size distribution changes to more random. It is likely that increment of the temperature influences the ionic migration and accelerates the generation and dissolution rate of ZnO in varying proportions. As a consequence, the generation and dissolution balance of ZnO nanoparticles is influenced.

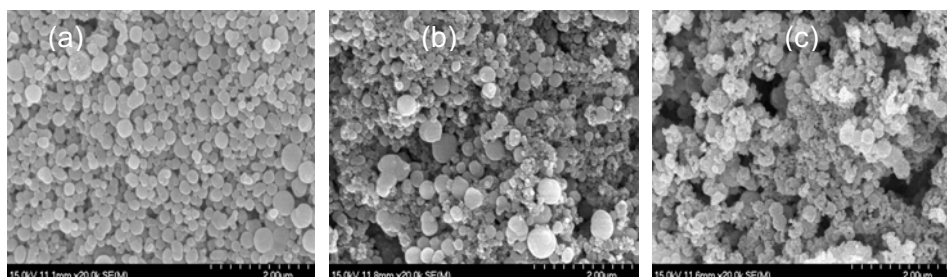
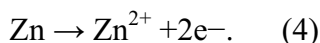


**Fig.4.** FE-SEM images of nano-ZnO prepared at different temperature. (a) 25°C (b) 35°C (c) 45°C.

Fig.5. shows the FE-SEM images of sample prepared in 1%  $\text{NH}_4\text{F}$ (quality score) solution ( $\text{H}_2\text{O}:\text{C}_2\text{H}_5\text{OH}$  1:1) at 25°C and 0.2M citric acid as pH regulator for 10 min with various anodization voltage. From these images it is seen that the influence of voltage seems to be more remarkable. The discal ZnO nanoparticles only can be formed at 40V anodization voltage. It is probably because the function of voltage is demonstrated in two aspects. First, voltage is the necessary driving force to the formation of  $\text{Zn}^{2+}$ :



At the initial stage of the reaction,  $Zn^{2+}$  is formed on the Zn foil as reaction(3) described. At high anodization voltages (50 V and 60 V), the electrochemical anodization speed was very fast. On the other hand, it can accelerate the movement of ions in solution perpendicular to the face of anode. As we have discussed above, the morphology of nano-ZnO species varies along with the speed of ionic movement. High anodization voltages (50V and 60V) enlarge the perpendicular speed, leading to various morphologies of nano-ZnO species.

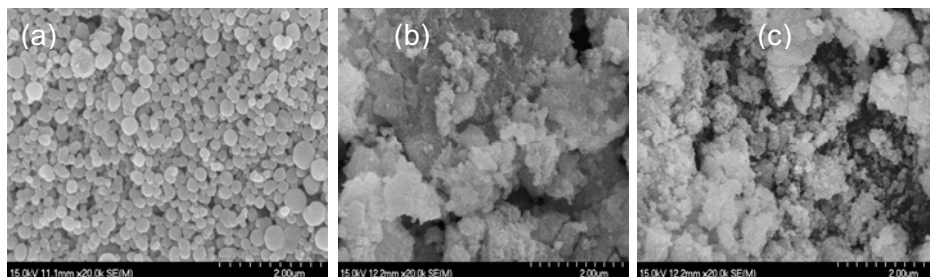


**Fig.5.** FE-SEM images of nano-ZnO prepared under different voltages. (a) 40V(b) 50V (c)60V

### 3.5 Photocatalytic Reduction Activity of CO<sub>2</sub>

The catalytic activity of ZnO was tested by the photocatalytic reduction of CO<sub>2</sub>. Transformation of the CO<sub>2</sub> to hydrocarbons is a positive direction to solve the lack of energy and the ever-increasing CO<sub>2</sub> concentration[21]. Much attention has been paid to semiconductor photocatalyst especially modified TiO<sub>2</sub> in recent years[22~24]. A single semiconductor does not effectively generate and separate electron-hole pairs. As a wide band gap semiconducting oxide, ZnO have been expected. Its energy gap a little greater than TiO<sub>2</sub> can reach to 3.3ev (Fig.6b) that bring in bigger reduction potential. The performance of ZnO is considered to be influenced by the nanoscale morphologies. The ZnO material with discal shaped nanoparctiles shows rather high photocatalytic reduction activity of CO<sub>2</sub> from Fig.6a. The yield of CH<sub>4</sub> reaches 2.48 umol/gcatalyst, which is as ten times as the other two samples. The efficiency of ZnO could expect to be further improved by altering the morphologies.

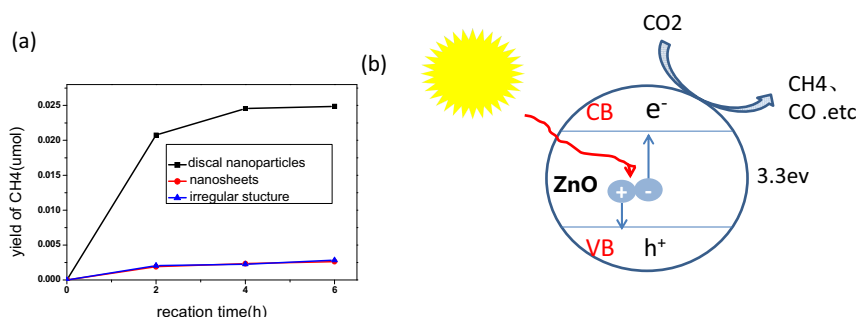


**Fig.6.** (a) yield of CH<sub>4</sub> with 0.01g different nano-ZnO structure as catalyst. (b) Schematic illustration of photoinduced generation of an electron–hole pair in ZnO semiconductor that catalyze CO<sub>2</sub> photoredox.

## 4 Conclusion

Nano ZnO material was fabricated by anodization process. The influence of the different anodization conditions, such as the pH regulator, the electrolyzer, the NH<sub>4</sub>F concentration, the temperature and voltage are investigated in detail. The morphology of as-prepared ZnO material was determined by the generation, the dissolution and the movement of nano-ZnO species during anodization. It is under the conditions of 0.2M citric acid as pH buffer, electrolyzer (H<sub>2</sub>O:C<sub>2</sub>H<sub>5</sub>OH 1:1), 1% NH<sub>4</sub>F (quality score), 25°C and 40V that a nano ZnO material with discal shaped nanoparticles is obtained. The ZnO material is supposed to be good for photon catalyst application due to its regular structures. It's the yield of CH<sub>4</sub> over the ZnO material can reach to 2.48 μmol/g in photocatalytic reduction of CO<sub>2</sub>.

## References

1. M. Guo, P. Diao, S. Cai, Hydrothermal growth of perpendicularly oriented ZnO nanorod array film and its photoelectrochemical properties, *Appl. Surf. Sci.* 249 (2005) 71-75.
2. W.J. Lee, A. Suzuki, K. Imeda, H. Okada, A. Wakahara, A. Yoshida, Fabrication and Characterization of Eosin-Y-Sensitized ZnO Solar Cell, *Jpn. J. Appl. Phys.* 143 (2004) 152-155.
3. M.H. Huang, S. Mao, H. Feick, H. Yan, Y. Wu, H. Kind, E. Weber, R. Russo, P. Yang, Room-Temperature Ultraviolet Nanowire Nanolasers, *Science* 292 (2001) 1897-1899.
4. B. Pal, M. Sharon, Enhanced photocatalytic activity of highly porous ZnO thin films prepared by sol-gel process *Mater. Chem. Phys.* 76 (2002) 82-87.
5. X.D. Bai, E.G. Wang, P.X. Gao, Z.L. Wang, Measuring the work function at a nanobelt tip and at a nanoparticle surface, *Nano Lett.* 3 (2003) 1147-1150.
6. J. Johnson, H. Yan, P. Yang, R. Saykally, Optical cavity effects in ZnO nanowire Lasers and Waveguides, *J. Phys. Chem. B* 107 (2003) 8816-8828.
7. S. Sreekantan, L. R. Gee, Z. Lockman, Room temperature anodic deposition and shape control of one-dimensional nanostructured zinc oxide. *J. Alloys Compd.* 476(2009) 513-518.
8. L.T. Canham, Silicon quantum wire array fabricated by electrochemical and chemical dissolution of wafers, *Appl. Phys. Lett.* 57 (1990) 1046-1048.
9. O. Jessensky, F. Muller, U. Gosele, Self-organized formation of hexagonal pore arrays in anodic alumina, *Appl. Phys. Lett.* 72 (1998) 1173-1175.
10. D. Gong, C.A. Grimes, O.K. Varghese, W. Hu, R.S. Singh, Z. Chen, E.C. Dickey, Titanium oxide nanotube arrays prepared by anodic oxidation, *J. Mater. Res.* 16 (2001) 3331-3334.
11. J. M. Macak, H. Tsuchiya and P. Schmuki, High-aspect-ratio TiO<sub>2</sub> nanotubes by anodization of titanium, *Angew. Chem. Int. Ed.* 44 (2005) 2100-2102.
12. H. Tsuchiya, J.M. Macak, I. Sieber, L. Taveira, A. Ghicov, K. Sirotna, P. Schmuki, Self-organized porous WO<sub>3</sub> formed in NaF electrolytes, *Electrochem. Commun.* 7 (2005) 295-298.
13. H. Tsuchiya, P. Schmuki, Self-organized high aspect ratio porous hafnium oxide prepared by electrochemical anodization, *Electrochem. Commun.* 7 (2005) 49-52.
14. I. Sieber, H. Hildebrand, A. Friedrich, P. Schmuki, Formation of self-organized niobium porous oxide on niobium, *Electrochem. Commun.* 7 (2005) 97-100.

15. S.J. Kim, J. Lee, J. Choi, Understanding of anodization of zinc in an electrolyte containing fluoride ions, *J. Electrochim. Acta.* 53(2008) 7941-7945.
16. S.J. Kim, J. Choi, Self-assembled arrays of ZnO stripes by anodization, *Electrochem. Commun.* 10 (2008) 175-179.
17. S.S. Chang, S.O. Yoon, H.J. Park, A. Sakai, *Appl. Surf. Sci.* Luminescence properties of anodically etched porous Zn, 158 (2000) 330-334.
18. M. Izaki, Preparation of transparent and conductive zinc oxide films by optimization of the two-step electrolysis technique, *J. Electrochem. Soc.* 146(1999) 4517-4521.
19. C.Y. Kuan, J.M. Chou, I.C. Leu, M.H. Hon, Formation and field emission property of single-crystalline Zn microtip arrays by anodization, *Electrochem. Commun.* 9 (2007) 2093-2097.
20. C.A. Grimes, G.K. Mor, Fabrication of TiO<sub>2</sub> nanotube arrays by electrochemical anodization: four synthesis generations, in: *TiO<sub>2</sub> Nanotube Arrays*, Springer, 2009, pp. 1-66.
21. C. Wang, J. Li, L. Xu, Reduction of CO<sub>2</sub> aqueous solution by using photosensitized-TiO<sub>2</sub> nanotube catalysts modified by supramolecular metalloporphyrins-ruthenium(II) polypyridyl complexes. *J. Mol. Catal. A-Chem.* 363 (2012) 108-114.
22. M. Reli, K. Kamila, M. Vlastimil, K. Pavel, O. Lucie, Effect of calcination temperature and calcination time on the kaolinite/TiO<sub>2</sub> composite for photocatalytic reduction of CO<sub>2</sub>, *GeoSci. Eng.* 58 (2012) 10-22.
23. K. Satoshi, K. Hidekazu, O. Kiyohisa, M. Takayuki, S. Akira, Photocatalytic reduction of CO<sub>2</sub> using TiO<sub>2</sub> powders in liquid CO<sub>2</sub> medium, *J. Photochem. Photobiol. A* 109 (1997) 59-63.
24. C.J. Wang, R.L. Thompson, J. Baltrus, C. Matranga, Visiblelight photoreduction of CO<sub>2</sub> using CdSe/Pt/TiO<sub>2</sub> heterostructured catalysts, *J. Phys. Chem. Lett.* 1 (2010) 48-53.